VI-D Synchrotron Radiation Stimulated High-Speed Etching on Silicon Surfaces

Synchrotron radiation (SR) stimulated process (etching, CVD) has excellent characteristics of unique material selectivity, low damage, low contamination, high spatial resolution and high precision, *etc*. We have utilized these advantages for silicon and silicon oxide substrates fabrication for bio-sensing devices. However, the slow etching rate in the SR-stimulated etching process is the bottle-neck for the through-hole type device fabrication. In this project, we are constructing a new SR-etching system using XeF_2 gas as a etching gas, in order to achieve high-speed SR-etching.

VI-D-1 Construction of High-Speed Synchrotron Radiation Etching System Using XeF_2

NAKAI, Naohito[1]; CHIANG, Tsung-Yi; UNO, Hidetaka; TERO, Ryugo; SUZUI, Mitsukazu; TERAOKA, Yuden[2]; YOSHIGOE, Akitaka[2]; MAKIMURA, Tetsuya[3]; MURAKAMI, Kouichi[3]; URISU, Tsuneo
([1]SOKENDAI; [2]JAEA; [3]Univ. Tsukuba)

We have been constructing a new synchrotron radiation (SR) induced high-speed etching system to make a through-hole type biosensor on Si substrates. The conventional SR-etching using SF_6 has the etching rate of only ~2 nm min^{-1} (at 200 mA ring-current), therefore is not suitable for micrometer-order deep etching. XeF_2 is known as an etching gas for the high-speed vapor-phase etching and is used in the MEMS and μTAS fields. XeF_2 etching has, however, several disadvantages such as; an isotropic etching without directivity; material limitation, for example SiO_2 can not be etched. We expect that SR-induced etching under XeF_2 leads to the high-speed etching with good directivity. We constructed a new etching chamber with LiF window (Figure 1a), and equipped it to the UVSOR-BL4A1. The diagonal mirrors in the beam line will be adjusted to cut off the Li absorption band.

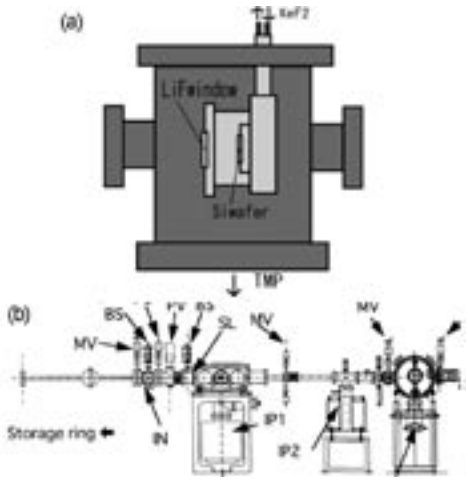

Figure 1. Schematic drawings of (a) the SR-induced XeF_2 etching chamber, and (b) the beam line equipped with the chamber (a).

VI-D-2 Vapor-Phase Etching of Silicon Substrates Using XeF_2

CHIANG, Tsung-Yi; NAKAI, Naohito[1]; UNO, Hidetaka; TERO, Ryugo; SUZUI, Mitsukazu; TERAOKA, Yuden[2]; YOSHIGOE, Akitaka[2]; MAKIMURA, Tetsuya[3]; MURAKAMI, Kouichi[3]; URISU, Tsuneo
([1]SOKENDAI; [2]JAEA; [3]Univ. Tsukuba)

XeF_2 vapor etching without SR irradiation was performed to check our XeF_2 flow system. Test pattern of a photoregist (N-HC600) was deposited on a Si substrate, and exposed to the 300 Pa of XeF_2 for 10–120 min. Figure 1a is the SEM image of the Si substrate after the photoregist removal. The image clearly shows that isotropic etching by XeF_2 has proceeded. Figure 1b shows the line profile of the line-and space pattern with 50 μm width after the XeF_2 etching, measured by a non-contact three-dimensional measurement instrument. The etching rate of 900 nm min^{-1} was obtained.

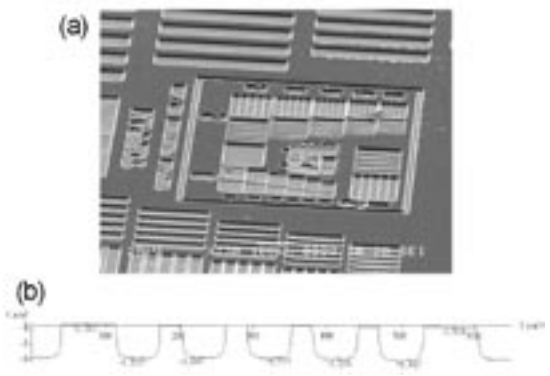

Figure 1. (a) SEM image of the Si substrate after the exposure to 300 Pa of XeF_2 for 10 min. (b) Non-contact three-dimensional measurement profile of the 50 μm wide line-and-space patterns on the Si substrate shown in (a).

VI-E Fabrication of Silicon-Based Planar Ion-Channel Biosensors

It is known that more than 50% of target proteins in the drag discovery field based on the genome information are membrane proteins. The patch clamp method is a powerful and widely used technique for the membrane protein studies, but is not suitable for the high-throughput and multi-integrated screening application. In this project, we have constructed a through-hole silicon device for the ion-channel biosensors. We succeeded to fabricate low-noise planer-type silicon device, and to detect the single ion channel current of gramicidin A.

VI-E-1 Fabrication of Circular Through-Hole on Si(100)-SOI Substrate

ZHANG, Zhen-Long[1]; UNO, Hidetaka; CHIANG, Tsung-Yi; ASANO, Toshifumi[1]; SUZUI, Mitsukazu; TERO, Ryugo; NAKAO, Satoshi; URISU, Tsuneo
([1]SOKENDAI)

We have fabricated a circular through-hole on Si(100)-SOI substrate for channel current measurement. The through-hole is necessary for the electronic conduction, and the circular hole with sharp edge is important for the lipid bilayer membrane formation over the hole and the membrane stability. Figure 1 shows the substrate fabrication process. The Si (100)-SOI (600 μm thick) (Figure 1a) substrate was annealed at water-saturated O_2 flow at 950 °C for 2 h to form a 200 nm thick thermally oxidized layer (Figure 1b). A circular hole with depth of ~550 μm was made by a diamond grinder on the back-side surface of the Si(100)-SOI (Figure 1c). Then the hole was etched in tetramethyl ammonium hydroxide (TMAH) until the hole reached to the oxide layer in SOI (Figure 1d). After a 20 nm thick SiO_2 layer was deposited on the top-side surface by sputtering (Figure 1e), the 2–3 μm thick SiO_2/Si(100) layer was penetrated by focused ion beam (FIB) (Figure 1f). The diameter of the hole can be controlled in the range of 1–100 μm. Figure 2 shows the optical microscope image of the through-hole with 100 μm diameter. The through-hole made by the processes shown in Figure 1 had a perfect circular shape and a shape edge.

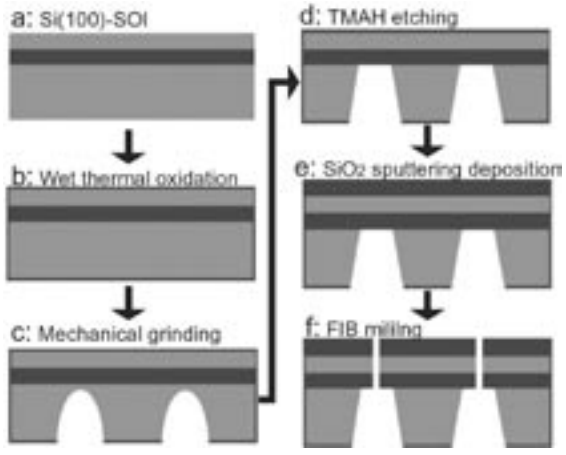

Figure 1. Schematic drawings of the through-hole fabrication processes on a Si(100)-SOI substrate.

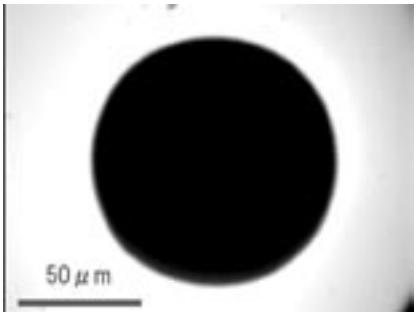

Figure 2. Optical microscope image of the through-hole with 100 μm diameter made by the processes shown Figure 1.

VI-E-2 Channel Current Measurement Using Silicon-Based Planar Type Biosensor

UNO, Hidetaka; ZHANG, Zhen-Long[1]; ASANO, Toshifumi[1]; CHIANG, Tsung-Yi; SUZUI, Mitsukazu; TERO, Ryugo; NAKAO, Satoshi; NONOGAKI, Youichi; URISU, Tsuneo
([1]SOKENDAI)

We have formed a suspended phospholipid bilayer membrane on the Si(100)-SOI through-hole chip (Figure 1), and measured the channel current of gramicidin A (gA). We deposited octadecyltrimethoxysilane by chemical vapor deposition to make the oxidized layer surface of the chip hydrophobic. The through-hole chip was settled in a home-build Teflon chamber, and the suspended bilayer of diphytanoylphosphatidylcholine (DøPC) was formed in the hole by painting method using 10 mg/ml of DøPC/decane solution. The electrical property of the bilayer membrane was measured by a patch clamp amplifier (CEA-2400, Nihon Koden, Japan). Aqueous gA solution was added to the both sides of the bilayer, to reconstitute the gA in to the bilayer. We succeeded in measuring the single channel current of gA using the through-hole silicon chip (Figure 2). Each of the step-signal in Figure 2 is the single channel current thorough gA.

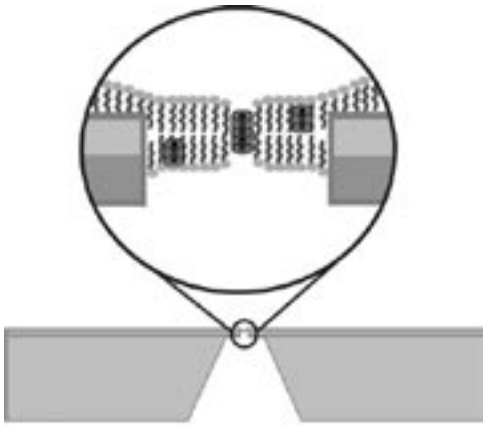

Figure 1. Schematic drawing of the through-hole silicon chip and the suspended lipid bilayer containing gA in the hole.

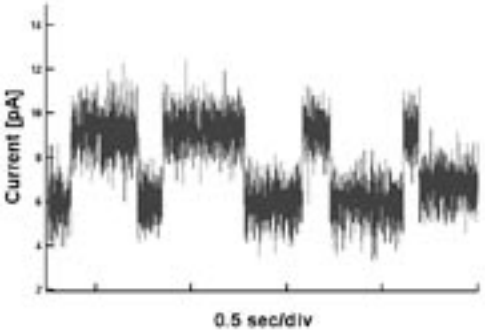

Figure 2. Single ion channel current signals of gA measured by the through-hole silicon chip. Bias voltage is 150 mV.

VI-E-3 Noise Analysis in the Planar-Type Ion-Channel Biosensors

UNO, Hideteka; ZHANG, Zhen-Long[1]; CHIANG, Tsung-Yi; SUZUI, Mitsukazu; TERO, Ryugo; NAKAO, Satoshi; NONOGAKI, Youichi; URISU, Tsuneo
([1]SOKENDAI)

[*Jpn. J. Appl. Phys.* submitted]

Low noise electronic systems in pA order is necessary for the ion channel current detection from single molecule. It has been believed that silicon is an inept material in ion channel detecting, because its high dielectric loss causes high noise level. However, our through-hole silicon chip during the gA channel measurement showed sufficiently low noise level (1.7 pA, rms). We investigated the noise sources in our silicon chip based on the dimension parameters shown in Figure 1. The main noise sources in planar bilayer recordings are; (1) I_h: the current noise from the interaction between the head-stage input voltage noise (e_n) and the input capacitance (C_t); (2) I_{Ra}: the current noise due to the thermal voltage noise of the access resistance R_a in series with the bilayer capacitance C_m; (3) I_d: the dielectric noise. These noise variances are expressed as

$$I_h^2 = (4/3)e_n^2 \pi^2 C_t^2 B^3 \quad (1),$$
$$I_{Ra}^2 = (4/3)k T R_a (2\pi C_m)^2 B^3 \quad (2),$$
$$I_d^2 = 4k T \pi D C_t B^2 \quad (3),$$
$$C_t = C_m + C_{sub} + C_{others} \quad (4),$$

where B is the frequency band width, C_{sub} is the capacitance of the substrate, C_{others} is the sum of other capacitances contributing to noise. The measured noise current I_m is given by

$$I^2 = I_h^2 + I_{Ra}^2 + I_d^2 \quad (5).$$

We calculated these capacitance and noise current values based on the substrate structure used in our experiments shown in Figure 1. The calculated values in B =5 kHz are; C_m = 76 pF; C_{sub} = 2 pF; C_{others} = 1.2 pF; C_t = 80 pF; $I_h^2 = 5.5 \times 10^{-26}$ A^2 (assuming $e_n = 2.3 \times 10^{-9}$ V Hz$^{0.5}$); R_a = 1.7 kΩ; and $I_{Ra}^2 = 2.7 \times 10^{-25}$ A^2. Thus the calculated noise current I = 1.7 pA (rms) was obtained. This value is in quite good agreement with the measured value 1.2 pA. We found that the SiO_2 disk around the hole (C_1 region in Figure 1) contributed to the low noise level in our chip.

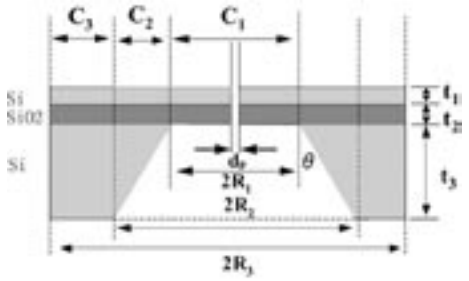

Figure 1. Schematic drawing of the through-hole silicon chip and its dimension parameters.

VI-F Integration and Characterization of Bio-Functional Materials on Silicon Surfaces

Integration of bio-functional materials on solid surfaces is an attractive research theme and important to the development of new biosensors and screening methods in which biological reactions are directly detected on electronic circuits. We have investigated the lipid bilayer membrane deposition and covalent immobilization of protein, and have characterized the properties of these bio-functional materials using atomic force microscopy infrared absorption spectroscopy. We have also developed a new infrared absorption spectroscopy system using buried-metal-layer substrate, for the in-situ measurements of water/solid interface.

VI-F-1 Supported Phospholipid Bilayer Formation on Hydrophilicity-Controlled Silicon Dioxide Surfaces

TERO, Ryugo; WATANABE, Hidekazu[1]; URISU, Tsuneo
([1]RIKEN)

[*Phys. Chem. Chem. Phys.* **8**, 3885–3894 (2006)]

We investigated the influence of surface hydroxyl groups (-OHs) on the supported planar phospholipid bilayer (SPB) formation and characteristic. We prepared SiO_2surfaces with different hydrophilicity degree by annealing the SiO_2 layer on Si(100) formed by wet chemical treatments. The hydrophilicity reduced with irreversible thermal desorption of -OHs. We formed SPB of dimyristoylphosphatidylcholine (DMPC) on the SiO_2 surfaces by incubation at a 100-nm-filtered vesicle suspension. The formation rate was faster on less hydrophilic surfaces (Figure 1). We proposed that a stable hydrogen-bonded water layer on the SiO_2 surface worked as a barrier to prevent vesicle adhesion on the surface. Theoretical calculation indicates that water molecules on vicinal surface -OHs take a stable surface-unique geometry, which disappears on an isolated -OH. The surface -OH density, however, little affected the fluidity of once formed SPBs, which was measured by the fluorescence recovery after photobleaching method. We also describe about the area-selective SPB deposition using surface patterning by the focused ion beam.

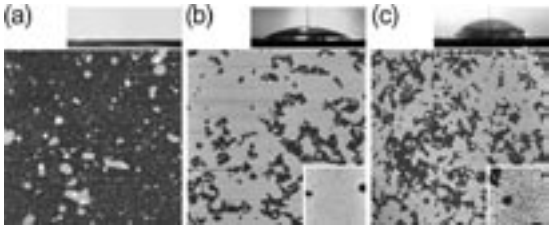

Figure 1. AFM images of DMPC-SPB on hydrophilicity-controlled SiO_2/Si(100) surfaces. The water contact angle of the SiO_2 surfaces before the DMPC deposition and the SPB coverage are; (a) 5°, 0.12; (b) 24°, 0.78; and (c) 67°, 0.67, respectively. The AFM images were obtained in a buffer solution.

VI-F-2 Orientation of Avidin Molecules Immobilized on COOH-Modified SiO_2/Si(100) Surfaces

MISAWA, Nobuo; YAMAMURA, Shusaku[1]; KIM, Yong-Hoon[1]; TERO, Ryugo; NONOGAKI, Youichi; URISU, Tsuneo
([1]SOKENDAI)

[*Chem. Phys. Lett.* **419**, 86–90 (2006)]

Avidin molecules were immobilized on a COOH-modified SiO_2/Si(100) surface with sub-nanometer order flatness (root-mean-square (rms) roughness ~0.1 nm) forming covalent bonds between the COOH groups on the substrate surface and the NH_2 groups of avidin molecules. The structures of avidin-immobilized surfaces were investigated by atomic force microscopy (AFM), ellipsometry, and infrared (IR) reflection absorption spectroscopy using buried metal layer substrate (BML-IRRAS), and transmission IR absorption spectroscopy (TIRAS). We have simulated dependence of the amide I band intensity on the avidin orientation (Figure 1), since BML-IRRAS and TIRAS are sensitive to perpendicular and parallel dipole moments to the surface, respectively. These data have evidenced that the avidin molecules are immobilized with the 2-fold symmetry axis of the tetramer almost perpendicularly to the substrate surface.

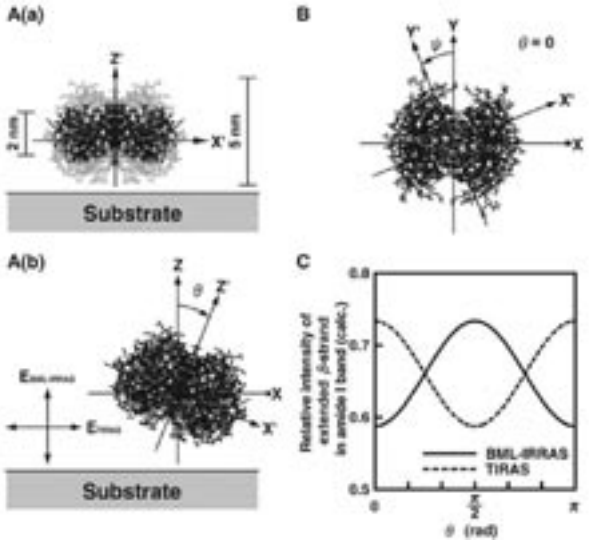

Figure 1. Schematic images of an egg white avidin molecule immobilized on the substrate surface. All component atoms are plotted using the coordinate data given in PDB (1AVD) as dots of the same size in A(a): avidin tetramer (gray) and the only β-barrel part (dark). Coordinates *X*, *Y* and *Z* are fixed to the substrate surface, while *X*', *Y*' and *Z*' are fixed to the molecule. Molecular orientation is defined by the Eulerian angles, φ (= 0), θ and ψ in A(b) and B. Electric fields, $E_{\text{BML-IRRAS}}$ and E_{TIRAS}, in BMLIRRAS and TIRAS are drawn in A(b). Calculated relative intensities of extended b-strand peak in the amide I band as a function of θ ($0 \le h \le \pi$) are shown in C.

VI-F-3 AFM Characterization of Gramicidin-A in Tethered Lipid Membrane on Silicon Surface

LEI, Sheng-Bin[1]; TERO, Ryugo; MISAWA, Nobuo; YAMAMURA, Shusaku[2]; WAN, Li-Jun[1]; URISU, Tsuneo
([1]IMS and Chinese Acad. Sci.; [2]SOKENDAI)

[*Chem. Phys. Lett.* in press]

The tethered 1,2-dipalmitoyl-*sn*-glycero-3-phosphocholine (DPPC) lipid bilayer is formed on the oxidized Si surfaces using the avidin-biotin interaction to investigate the lipid-membrane protein interactions by using gramicidin-A (g-A) as a model membrane protein. The morphology of the tethered lipid bilayer, observed by the *in situ* atomic force microscopy (AFM), changes drastically by the reconstruction of g-A (Figure 1). The aggregation behavior of g-A is clearly different in the tethered membrane from those in the simple supported

membranes on mica and SiO_2 surfaces. The thick water layer under the membrane introduced by the tethered structure gives important influence on the aggregation behavior of g-A.

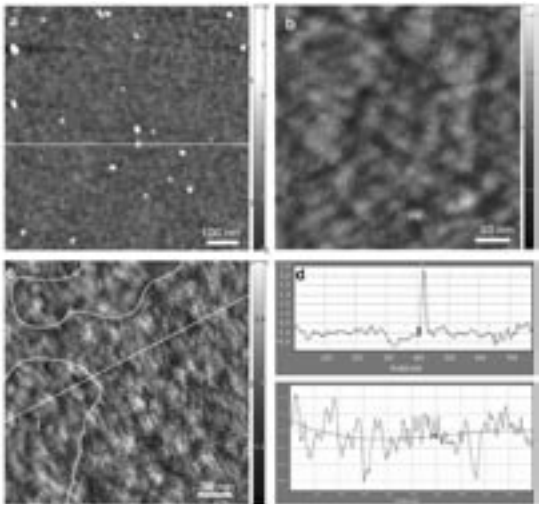

Figure 1. Topography images of (a) avidin immobilized substrate, and tethered lipid bilayers (b) without and (c) with 1 mol% g-A. (d) The line profile of marked place in (a) and (c). Color scales are (a) 7.5 nm, (b) 1.7 nm and (c) 1.5 nm full scale.

VI-F-4 In-Situ Infrared Reflection Absorption Spectroscopy System Using Buried Metal Layer Substrate (BML-IRRAS) for Biomaterials under Water

SAYED, Md. Abu[1]; UNO, Hidetaka; MISAWA, Nobuo; HARADA, Kensuke[2]; TANAKA, Keiichi[2]; KONDOH, Takuhiko; TERO, Ryugo; URISU, Tsuneo
([1]SOKENDAI; [2]Kyushu Univ.)

Supported membrane on biosensor surface is one of the most attractive research fields in these days. For new bioactive biosensor or biochips for diagnostics or other electronic purposes we have to study biomaterial properties on solid surfaces in different conditions. Many experimental approaches including infrared reflection absorption spectroscopy using buried metal layer (BML-IRRAS) have been performed to study the function of biomaterials on inorganic surfaces. But there are few IRRAS techniques to study the membrane surface reaction under aqueous solution. We have constructed a new BML-IRRAS system to study biomaterials under water. We used CaF_2 prism and 12 μm aluminum spacer upon BML substrate including a solution injection system (Figure 1a). We used JIR-7000 (JEOL Ltd.) with a MCT detector as a FT-IR system. Although water is necessary for biomaterials to keep life functions, but water have strong absorptivity in the IR region. We have investigated the window regions for H_2O and D_2O as shown in Figure 1b. It is concluded that 1250–4000 cm^{-1} and 3700–4000 cm^{-1} are applicable for IR measurements in D_2O and H_2O, respectively, in the present system.

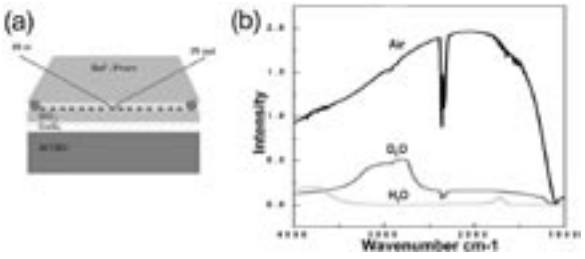

Figure 1. (a) Schematic drawings of the sample holder for the new BML-IRRAS system. (b) IR power spectra measured by the new BML-IRRAS instrument for (a) air, (b) D_2O and (c) H_2O with 12 nm thickness.